



A Non-Oscillatory Scheme for the One-Dimensional SABR Model

Nawdha Thakoor

Department of Mathematics, University of Mauritius, Reduit, Mauritius

ABSTRACT

The Stochastic Alpha Beta Rho (SABR) is a popular stochastic volatility model for pricing interest rate derivatives. In contrast to local volatility models, the SABR model correctly captures the movement of the volatility smile. The model's density can be approximated by the solution of a one-dimensional partial differential equation (pde). Solving for the density using the Crank-Nicolson discretisation results in loss of accuracy in computation of European option prices. This paper proposes a non-oscillatory scheme for approximating the density function using an exponential time integration scheme. The non-oscillatory property leads to an efficient scheme for option valuation via quadrature of the density function. Numerical examples illustrate that European option prices can be computed with high accuracy.

Keywords: CEV, exponential time integration, Quadrature, SABR, volatility smiles and skews

INTRODUCTION

The implied volatility surface computed by inversion of the Black-Scholes formula with respect to market option prices is strike and maturity dependent. Due to the inability of the constant volatility Black-Scholes model to fit the implied volatility surface, an important derivative pricing problem is the development of efficient procedures for pricing of options under a model with capability of fitting a volatility skew, a decreasing shape with the option's strike price or under a model consistent with a smile, a u-shaped volatility profile. The constant elasticity of variance (CEV) process (Schroder, 1989) in which the local instantaneous volatility is a function

of the strike price and its stochastic extension known as the Stochastic Alpha Beta Rho (SABR) model (Hagan, Kumar, Lesniewski, & Woodward, 2002) are two popular models for pricing options consistent with market smiles and skews.

The CEV model has the capability of fitting the volatility skew and has the

ARTICLE INFO

Article history:

Received: 05 June 2017

Accepted: 23 September 2017

E-mail address:

n.thakoor@uom.ac.mu (Nawdha Thakoor)

advantage that the pricing equation is one-dimensional. Efficient methods for option pricing under the CEV model can be found in Thakoor, Tangman, & Bhuruth (2013, 2014, 2015). The SABR model is one of the most widely accepted stochastic volatility model for modelling the smile shaped volatility surface. The model's implied volatility approximation leads to an easy computation of European option prices (Hagan et al., 2002) and American option prices (Chang, Chung, & Stapleton, 2007). However, the asymptotic expansion formula for the implied volatility has two drawbacks. First, for long-maturity options with low strike prices, the implied volatility used to compute option prices leads to the possibility of arbitrage and second, at the lower boundary, there exists a boundary layer which can significantly affect the option price (Hagan, Kumar, Lesniewski, & Woodward, 2014).

Paulot (2015) proposed some improvements based on second-order expansions to the original formula but stated that for long maturities, unless a valid long maturity expansion could be found, a numerical method is more appropriate. A comparison of different improvements can be found in Oblój (2008). Andreasen & Huge (2012) proposed an arbitrage-free 'SABR-like' model where the implied volatility formula converges with the Hagan formula for short maturities but for larger maturities, the solutions are different. Balland & Tran (2013) proposed a method which eliminates arbitrage in the lower strike wing by a normal volatility expansion with absorption at zero. An exact formula was introduced by Antonov, Konikov, & Spector (2013) for pricing European call options under the SABR model for the case when the Brownian motions of the forward price and volatility are uncorrelated.

Then for the correlated cases, these authors showed that the SABR model parameters can be mapped to an uncorrelated model. This method is near-arbitrage but the pricing is slower than that of Hagan as for the correlated case, the mapping of the volatility parameter is strike dependent which makes the pricing process expensive.

The SABR model leads to a two-dimensional pde for the pricing of options. Using asymptotic techniques, Hagan et al. (2014) reduced the two-dimensional SABR density to a one-dimensional equation for the probability density of the forward price. The authors then used a moment preserving Crank-Nicolson scheme to approximate the density. This scheme gives oscillatory solutions and in the case of the CEV model, we show that the computed density is not accurate enough and can result in mispricing. We developed a superior alternative using an exponential time integrator to show that convergence is fast and the scheme produces non-oscillatory solutions.

An outline of this paper is as follows: First, the SABR model and Hagan's analytical formula is reviewed in section 2. In section 3, the one-dimensional SABR equation for the density function is derived while in section 4, the numerical discretisation for the one-dimensional pde is provided. In section 5, numerical results for the pricing of European options are described to illustrate the merit of the paper's proposed scheme. The final section concludes the paper by summarising the main points.

The SABR Model

The SABR model (Hagan et al., 2002) extends the constant elasticity of variance model with a stochastic volatility process. In the constant elasticity of variance model, the volatility is

assumed to be locally constant while the SABR model allows the volatility to evolve as a function of time, the strike price and the forward price.

Letting α_t be the volatility of the forward price $F_t = S_0 e^{(r-q)(T-t)}$ where S_0 is the initial stock price, r is the risk-free rate, q is the dividend yield, the SABR model is described by the system of stochastic differential equations

$$\begin{aligned} dF_t &= \alpha_t F_t^\beta dW_t^1, & F_0 &= f, \\ d\alpha_t &= \nu \alpha_t dW_t^2, & \alpha_0 &= \alpha, \end{aligned} \tag{1}$$

where dW_t^1 and dW_t^2 are two correlated Wiener processes with correlation of ρ such that

$$dW_t^1 dW_t^2 = \rho dt,$$

where ν is the constant volatility of the volatility parameter, $0 \leq \beta \leq 1$ is the exponent parameter and W_t is a standard \mathbb{Q} -Brownian motion. Choosing $\nu = 0$ gives the CEV model for $0 \leq \beta \leq 1$, and for $\beta = 1$ and $\nu = 0$, we obtain the Black-Scholes model. In the SABR model, the volatility process is allowed to be random through the development of α_t , which is scaled up by including the factor volatility of volatility parameter, ν . This extra randomness solves the problem of constant volatility, which is an unrealistic assumption of the Black-Scholes model.

Analytical Approximations under SABR

By carrying out a small volatility expansion for the singularly-perturbed SABR model given by

$$\begin{aligned} d\tilde{F}_t &= \varepsilon \tilde{\alpha}_t \tilde{F}_t^\beta dW_t^1, & \tilde{F}_0 &= f, \\ d\tilde{\alpha}_t &= \varepsilon \nu \tilde{\alpha}_t dW_t^2, & \tilde{\alpha}_0 &= \alpha, \end{aligned} \tag{2}$$

where $\varepsilon \ll 1$ is the singular perturbation parameter which is eventually set to one, Hagan et al. (2002) showed that an analytical approximation to the implied volatility formula $\sigma_B(E, f)$ is given by

$$\begin{aligned} \sigma_B(E, f) &= \frac{\alpha \left[1 + \left(\frac{(1-\beta)^2 \alpha^2}{24(fE)^{1-\beta}} + \frac{\rho\beta\nu\alpha}{4(fE)^{(1-\beta)/2}} + \frac{(2-3\rho^2)\nu^2}{24} \right) T \right]}{(fE)^{(1-\beta)/2} \left(1 + \frac{(1-\beta)^2}{24} \left(\ln \frac{f}{E} \right)^2 + \frac{(1-\beta)^4}{1920} \left(\ln \frac{f}{E} \right)^4 \right)} \\ &\quad \times \frac{z}{w(z)}, \end{aligned} \tag{3}$$

where

$$z = \frac{\nu}{\alpha} (fE)^{\frac{1-\beta}{2}} \ln \left(\frac{f}{E} \right), \quad w(z) = \ln \left(\frac{\sqrt{1-2\rho z+z^2}+z-\rho}{1-\rho} \right).$$

In the case of the CEV model, the Hagan & Woodward (1999) implied volatility expression to first-order maturity is given by

$$\sigma_B^{CEV}(E, f) = \tilde{\sigma} \times \left(1 + \frac{(1 - \beta)(2 + \beta)(f - E)^2}{96(f + E)^2} + \frac{(1 - \beta)^2 \tilde{\sigma}^2 T}{24} \right), \tag{4}$$

where $\tilde{\sigma} = \alpha \left(\frac{1}{2}(f + E) \right)^{\beta - 1}$.

The time zero price of European options with maturity T and strike E on a forward contract can be expressed by Black's formula

$$V_{\text{call}} = e^{-rT} [f\Phi(d_+) - E\Phi(d_-)],$$

$$V_{\text{put}} = V_{\text{call}} + e^{-rT} [E - f],$$

where

$$d_{\pm} = \frac{\ln\left(\frac{f}{E}\right) \pm \frac{1}{2}\sigma_B^2 T}{\sigma_B \sqrt{T}},$$

and Φ is the cumulative distribution function of the standard normal distribution.

METHODOLOGY

The One-Dimensional Problem

By considering the singularly perturbed SABR model given by (2), Hagan et al. (2014) obtained a one-dimensional pde for the probability density function $Q(F, t)$ of the forward price on $F_{\min} < F < F_{\max}$ given by

$$Q(F, t)dF = \mathbb{P}(F < \tilde{F}(t) < F + dF | \tilde{F}(0) = f, \tilde{\alpha}(0) = \alpha_0).$$

They showed that $Q(F_{\min}, t) = Q_L(t)$, $Q(F_{\max}, t) = Q_R(t)$ and for $F_{\min} < F < F_{\max}$, the density $Q^c(F, t)$ is the solution of the diffusion

$$\frac{dQ^c}{dt} = \frac{1}{2}\varepsilon^2 \frac{\partial^2}{\partial F^2} (D^2(F)G(F, t)Q^c), \quad 0 \leq t \leq T, \tag{5}$$

where

$$D(F) = \sqrt{\alpha^2 + 2\alpha\rho\nu y(F) + \nu^2 y^2(F)F^\beta},$$

$$y(F) = \frac{F^{1-\beta} - f^{1-\beta}}{1 - \beta},$$

$$G(F, t) = e^{\rho\nu\alpha\Gamma(F)t}, \quad \Gamma(F) = \frac{F^\beta - f^\beta}{F - f},$$

with the initial condition given by

$$Q^c(F, t) \rightarrow \delta(F - f) \text{ as } t \rightarrow 0^+,$$

where δ is the Dirac delta function. The probability sums to one for all t , that is,

$$Q_L(t) + \int_{F_{\min}}^{F_{\max}} Q^c(F, t) dF + Q_R(t) = 1. \tag{6}$$

On differentiating (6) with respect to t and substituting (5) yields

$$\frac{dQ_L}{dt} = \lim_{F \rightarrow F_{\min}^+} \frac{1}{2} \varepsilon^2 \frac{\partial^2}{\partial F^2} (D^2(F)G(F, t)Q^c(F, t)), \tag{7}$$

$$\frac{dQ_L}{dt} = - \lim_{F \rightarrow F_{\max}^-} \frac{1}{2} \varepsilon^2 \frac{\partial^2}{\partial F^2} (D^2(F)G(F, t)Q^c(F, t)), \tag{8}$$

at the boundaries with the initial conditions

$$Q_L(t) \rightarrow 0, \quad Q_R(t) \rightarrow 0, \quad \text{as } t \rightarrow 0^+.$$

For $\tilde{F}(t)$ to be martingale, we require

$$\begin{aligned} \mathbb{E}[\tilde{F}(t) | \tilde{F}(0) = f, \alpha(0) = \alpha_0] \\ = F_{\min} Q_L(t) \\ + \int_{F_{\min}}^{F_{\max}} F Q^c(F, t) dF + F_{\max} Q_R(t) = f. \end{aligned} \tag{9}$$

Differentiating (9) with respect to t and on evaluating the integral term, we obtain the absorbing boundary conditions at $F = F_{\min}$ and $F = F_{\max}$ given by

$$\lim_{F \rightarrow F_{\min}^+} D^2(F)G(F, t)Q^c(F, t) = 0, \tag{10}$$

$$\lim_{F \rightarrow F_{\max}^-} D^2(F)G(F, t)Q^c(F, t) = 0. \tag{11}$$

European call or put option prices can then be obtained by integrating the payoff against the terminal density

$$\begin{aligned} V_{\text{call}} &= (F_{\max} - E)Q_R(t) + \int_E^{F_{\max}} (F - E)Q^c(F, t) dF, \\ V_{\text{put}} &= (E - F_{\min})Q_L(t) + \int_{F_{\min}}^E (E - F)Q^c(F, t) dF. \end{aligned} \tag{12}$$

Given the martingale property (9) and the conservation of probability (6) the put-call parity

$$V_{\text{call}} - V_{\text{put}} = f - E,$$

holds exactly and thus, the computed option prices are arbitrage-free.

New Methodology

By localising problem (5) to the finite domain $(F_{\min}, F_{\max}) \times [0, T]$, the Hagan's scheme employs a moment preserving Crank-Nicolson discretisation. To describe this scheme, consider for $m = 0, 1, \dots, M + 1$, the intervals I_m given by

$$I_m = \left(F_m - \frac{h}{2}, F_m + \frac{h}{2} \right) \text{ where } F_m = F_{\min} + \left(m - \frac{h}{2} \right) h,$$

and the uniform mesh size $h = (F_{\max} - F_{\min})/M$ chosen in such a way that the initial forward price $f = F_{m_0}$ corresponds exactly to the midpoint of a cell I_{m_0} . Define the cell average $Q_m(t) = Q^c(F_m, t)$ by

$$Q_m(t) = \frac{1}{h} \int_{I_m} Q^c(F', t) dF', \quad \text{for } m = 1, 2, \dots, M.$$

A central-difference discretisation in space of (5) at the interior grid points is given by

$$(Q_t)_m = \frac{1}{2} \varepsilon^2 \delta_F^2 (D^2(F_m)G(F_m, t)Q_m(t)), \tag{13}$$

for $m = 1, 2, \dots, M$ where $\delta_F^2 U_m = (U_{m+1} - 2U_m + U_{m-1})/h^2$.

At the left boundary $F = F_{\min}$, the absorbing boundary (10) is implemented as the average of values on the left and right grid nodes. This gives

$$D^2(F_0)G(F_0, t)Q_0^c(t) = -D^2(F_1)G(F_1, t)Q_1^c(t). \tag{14}$$

Similarly, implementing the absorbing boundary condition (11) at $F = F_{\max}$, we obtain

$$D^2(F_{M+1})G(F_{M+1}, t)Q_{M+1}^c(t) = -D^2(F_M)G(F_M, t)Q_M^c(t). \tag{15}$$

Letting $\Delta_+ = (U_{(m+1)} - U_m)/h$ and $\Delta_- U_m = (U_m - U_{(m-1)})/h$, $Q_L(t)$ and $Q_R(t)$ are discretised as

$$Q'_L(t) = \frac{\varepsilon^2}{2} \Delta_+ [D^2(F_0)F(F_0, t)Q_0(t)],$$

$$Q'_R(t) = -\frac{\varepsilon^2}{2} \Delta_- [D^2(F_{M+1})F(F_{M+1}, t)Q_{M+1}(t)].$$

Let $\mathbf{Q}(t) = [Q_1(t), Q_2(t), \dots, Q_M(t)]^T$ denote the vector of the density values at time t . Then (13), (14) and (15) lead to the system of odes given by

$$\mathbf{Q}'(t) = \mathbf{D}\mathbf{G}(t)\mathbf{Q}(t), \tag{16}$$

where the matrix $\mathbf{D} \in \mathbb{R}^{M \times M}$ is tridiagonal and the matrix $\mathbf{G}(t) \in \mathbb{R}^{M \times M}$ is diagonal which are given by

$$\mathbf{D} = \begin{pmatrix} -3d_1 & d_2 & & & \\ d_1 & -2d_2 & d_3 & & \\ & d_2 & -2d_3 & d_4 & \\ & & \ddots & \ddots & \ddots \\ & & & d_{M-2} & -2d_{M-1} & d_M \\ & & & & d_{M-1} & -3d_M \end{pmatrix},$$

$$\mathbf{G} = \text{diag}[G_1(t), G_2(t), \dots, G_M(t)],$$

with

$$d_m = \frac{\varepsilon^2}{2h^2} D^2(F_m), \quad G_m(t) = G(F_m, t).$$

Then letting $\Delta t = T/N$, $\mathbf{I} \in \mathbb{R}^{M \times M}$ denote the identity matrix and applying a Crank-Nicolson time stepping gives

$$\left(\mathbf{I} - \frac{\Delta t}{2} \mathbf{D}\mathbf{G}^{n+1}\right) \mathbf{Q}^{n+1} = \left(\mathbf{I} + \frac{\Delta t}{2} \mathbf{D}\mathbf{G}^n\right) \mathbf{Q}^n, \tag{17}$$

for $n=0,1,\dots,N-1$, with the initial condition

$$\mathbf{Q}^0 = \frac{1}{h} \mathbf{1}_{m_0}^T, \tag{18}$$

where $\mathbf{1}_{m_0} \in \mathbb{R}^M$ is a vector with 1 in the m_0^{th} row and zero elsewhere. At each time step, the values of Q_L^{n+1} and Q_R^{n+1} are updated as

$$\begin{aligned} Q_L^{n+1} &= Q_L^n + \frac{h\Delta t}{2} (d_1 G_1^{n+1} Q_1^{n+1} - d_0 G_0^{n+1} Q_0^{n+1} + d_1 G_1^n Q_1^n - d_0 G_0^n Q_0^n), \\ Q_R^{n+1} &= Q_R^n - \frac{h\Delta t}{2} (d_{M+1} G_{M+1}^{n+1} Q_{M+1}^{n+1} - d_M G_M^{n+1} Q_M^{n+1} + d_{M+1} G_{M+1}^n Q_{M+1}^n \\ &\quad - d_M G_M^n Q_M^n). \end{aligned}$$

Now consider a put option with strike E . For $E < F_{\min}$, the option price $V_{\text{put}} = 0$ and for $E > F_{\max}$ the option price is given by $V_{\text{put}} = E - f$. For the case when $F_{\min} < E < F_{\max}$, suppose that E belongs to the interval (F_{k_0-1}, F_{k_0}) for some k_0 . Then, using (12), we find that

$$V_{\text{put}} = (E - F_{\min}) Q_L^N + h \sum_{m=1}^{k_0-1} (E - F_m) Q_m^N + Q_{k_0}^N \int_{F_{k_0-1} + \frac{h}{2}}^E (E - F) dF.$$

Evaluating the above integral gives

$$V_{\text{put}} = (E - F_{\min})Q_L^N + h \sum_{m=1}^{k_0-1} (E - F_m)Q_m^N + \frac{1}{2} \left(E - F_{k_0-1} - \frac{h}{2} \right)^2 Q_{k_0}^N.$$

Later in this paper, we show that the Crank-Nicolson scheme yields oscillatory solutions. To overcome this drawback of the Crank-Nicolson time stepping, we employ an exponential time integration for the semi-discrete system (16).

An exponential time integration scheme

An efficient alternative to the Crank-Nicolson scheme is an exponential time integration scheme (Cox & Matthews, 2002) which was first introduced in finance for option pricing in Tangman, Thakoor, Dookhitram, & Bhuruth (2011). Since only a single time step is required the algorithm can be very fast. Integrating the semi-discrete scheme (16) between 0 to T shows that

$$\ln \left(\frac{\mathbf{Q}(T)}{\mathbf{Q}(0)} \right) = \mathbf{D}\bar{\mathbf{G}},$$

where $\bar{\mathbf{G}} \in \mathbb{R}^{M \times M}$ is the diagonal matrix whose m^{th} diagonal element \bar{g}_m is given by

$$\bar{g}_m = \frac{G_m(T) - 1}{\rho\nu\alpha\Gamma(F_m)}.$$

Therefore, the computed density at time T is given by

$$\mathbf{Q}(T) = e^{\mathbf{D}\bar{\mathbf{G}}}\mathbf{Q}(0), \tag{20}$$

with the initial condition $\mathbf{Q}(0)$ given in (18). The left and right fluxes are then computed from

$$Q_L(T) = e^{-hd_0\bar{g}_0}Q_0(0) + e^{hd_1\bar{g}_1}Q_1(0),$$

$$Q_R(T) = e^{hd_M\bar{g}_M}Q_M(0) + e^{-hd_{M+1}\bar{g}_{M+1}}Q_{M+1}(0).$$

The matrix exponential in (20) can be computed using the ‘expm’ function in Matlab. However, this method uses Padé approximations which can lead to a computationally expensive algorithm for a large number of grid nodes.

The matrix exponential can be more efficiently evaluated using best rational approximations (Trefethen, 2007) and the Carathéodory–Fejér procedure (Trefethen & Gutknecht, 1983). Let γ be a Hankel contour and f be an analytic function on the neighbourhood of the negative real axis and consider the computation of the integral

$$I = \frac{1}{2\pi i} \int_{\gamma} e^z f(z) dz.$$

Let $\mathfrak{R}_\eta(z) = P(z)/Q(z)$ be a rational function, where P and Q are two polynomials of degree $n-1$ and n , that is a good approximation to e^z on $(-\infty, 0)$ and has poles at z_1, z_2, \dots, z_η with residues c_1, c_2, \dots, c_η . We can then obtain a good approximation to I given by

$$I_\eta = \frac{1}{2\pi i} \int_{Y'} \mathfrak{R}_\eta(z) f(z) dz,$$

where Y' is a contour lying between $(-\infty, 0)$. Expanding $\mathfrak{R}_\eta(z)$ in partial fractions given by

$$\mathfrak{R}_\eta(z) = \sum_{j=1}^{\eta} \frac{c_j}{z - z_j},$$

We obtain a quadrature formula for approximating the integral I which is given by

$$I_\eta = \sum_{j=1}^{\eta} c_j f(z_j),$$

Then if Y is a contour that encloses the spectrum of $D\bar{G}$, we have

$$e^{D\bar{G}} Q(0) = \frac{1}{2\pi i} \int_Y e^{sT} (sI - D\bar{G})^{-1} Q(0) ds,$$

where $I \in \mathbb{R}^{M \times M}$ is the identity matrix. Generalising $\mathfrak{R}_\eta(z)$ to the matrix $e^{D\bar{G}}$, a rational approximation to $e^{D\bar{G}} Q(0)$ can be obtained in terms of partial fraction expansion given by

$$e^{D\bar{G}} Q(0) \approx \sum_{j=1}^{\eta} c_j (D\bar{G} - z_j I)^{-1} Q(0).$$

The poles and residues appear in conjugate pairs since the discretisation matrix $D\bar{G}$ is a real tridiagonal matrix, which means that only $\eta/2$ tridiagonal solves are required for computing the price density which makes the proposed method achieve fast convergence.

To obtain the option price at the initial forward price for different strike prices, instead of using (19), we implement the formula (12) as

$$V_{\text{put}} = (E - F_{\text{min}}) Q_L(T) + \int_{F_{\text{min}}}^E (E - F) Q^c(F, t) dF, \tag{21}$$

where the finite integral in (21) can be obtained by using a numerical quadrature based on an adaptive Simpson method.

RESULTS AND DISCUSSION

We describe the results of some numerical examples for pricing European options, by first computing the density of the forward price. All numerical experiments have been performed using Matlab R2015a on a Core i5 laptop with 4GB RAM and speed 4.60 GHz.

Computed Black-Scholes and CEV Densities

Choosing $\nu=0$ and $\beta=1$ in (1) corresponds to the Black-Scholes model where the log-normal density is given by

$$Q_{bs}(F, T) = \frac{1}{F e^{-rT} \alpha \sqrt{2\pi T}} \exp\left(-\frac{(\ln F e^{-rT} - \mu)^2}{2\alpha^2}\right), \tag{22}$$

with $\mu = \ln(fe^{-rT}) + \left(r - \frac{1}{2}\alpha^2\right)T$ and the forward equation (5) reduces to

$$\frac{dQ^c}{dt} = \frac{1}{2}\alpha^2 \frac{\partial^2}{\partial F^2}(F^2 Q^c), \quad Q^c(F, t) \rightarrow \partial(F - t) \text{ as } T \rightarrow t.$$

We provide a numerical example which illustrates that the computed density using the one-dimensional equation (5), agrees well with the theoretical density (22). For this numerical example, we have chosen $f=20$, $F_{\max}=40$, $r=0.09$, $\alpha=0.25$ and a small maturity of $T=4/12$. The solutions computed by the Crank-Nicolson scheme (CN) and the ETD scheme (ETD) over the whole computational domain with $M=512$ spatial nodes for both methods and $N=40$ time steps for CN scheme are shown in Figure 1.

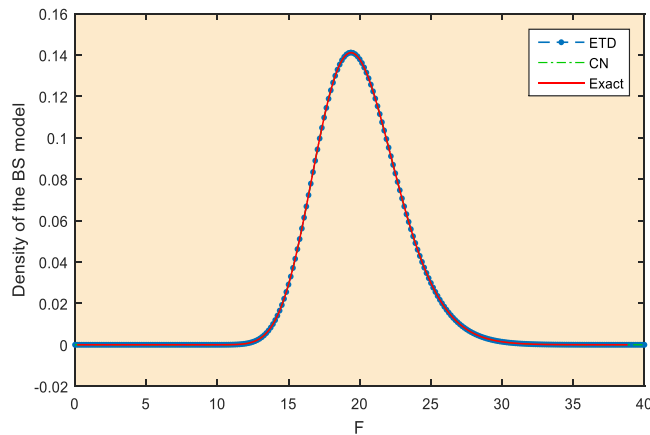


Figure 1. Computed CN, ETD and Exact Densities under the Black-Scholes Model

Table 1 shows that the density values computed by ETD are more accurate yielding a root mean square error (RMSE) of 10^{-8} while the density computed by CN gives a RMSE of 10^{-5} only.

Table 1
Black-Scholes density for different F

	$f = 20, r = 0.09, T = 4/12, \alpha_0 = 0.25$					RMSE
	F					
	14	18	20	22	26	
ETD	0.00111	0.12368	0.13784	0.09607	0.01782	
Error	6.0e-9	2.1e-9	5.0e-8	6.4e-9	9.9e-9	2.3e-8
CN	0.00112	0.12368	0.13789	0.09608	0.01781	
Error	6.8e-6	2.3e-7	5.3e-5	6.0e-6	1.0e-5	2.4e-5
Exact	0.00111	0.12368	0.13784	0.09607	0.01782	

Choosing $\nu = 0$ in (1), gives the CEV model for $0 \leq \beta \leq 1$, and the exact density function for the CEV model in terms of the forward price is given by

$$Q_{\text{CEV}}(F, T) = (2 - 2\beta)k^{2-2\beta} x^{\frac{1}{4-4\beta}} z^{1-\frac{5}{4(1-\beta)}} e^{-x-z} I_{\frac{1}{2-2\beta}}(2\sqrt{xz}), \tag{23}$$

where

$$k = \frac{1}{2\alpha^2 T(1-\beta)^2}, \quad x = kf^{2-2\beta}, \quad z = kF^{2-2\beta},$$

and $I_w(y)$ is the modified Bessel function of the first kind of order w given by

$$I_w(y) = \sum_{r=0}^{\infty} \frac{\left(\frac{y}{2}\right)^{2r+w}}{r! \Gamma(r+1+w)}.$$

For this model, the one-dimensional density pde (5) reduces to

$$\frac{dQ^c}{dt} = \frac{1}{2}\alpha^2 \frac{\partial^2}{\partial F^2}(F^{2\beta}Q^c), \quad Q^c(F, t) \rightarrow \partial(F-f) \text{ as } T \rightarrow t.$$

where $\alpha = \tilde{\sigma}f^{1-\beta}$.

In Figure 2, the exact density (23), computed CN and ETD densities are shown for the case when $\beta = 0$ and Table 2 gives the computed CN and ETD density values. The other parameters are chosen as $f = 100, T = 4, r = 0$ and $\tilde{\sigma} = 0.5$. The numerical example is performed using $M = 512$ spatial and $N = 40$ time steps with $F_{\text{max}} = 800$. A non-oscillatory and highly accurate density is obtained by the ETD scheme whereas the CN solution exhibits oscillations near the initial forward price.

Table 2
CEV Density for Different F and a Large Maturity

$f = 100, \beta = 0, r = 0, T = 4, \bar{\sigma} = 0.5$								
	F							
	70	90	100	110	130	200	400	RMSE
ETD	0.00287	0.00331	0.00345	0.00353	0.00353	0.00238	0.00004	
Error	1.5e-7	1.6e-7	1.5e-7	1.4e-7	1.0e-7	6.3e-8	1.3e-8	1.2e-7
CN	0.00287	0.00300	0.00741	0.00320	0.00353	0.00238	0.00004	
Error	9.6e-7	3.2e-4	3.9e-3	3.2e-4	9.7e-7	2.9e-8	2.5e-9	1.5e-3
Exact	0.00287	0.00331	0.00345	0.00353	0.00353	0.00238	0.00004	

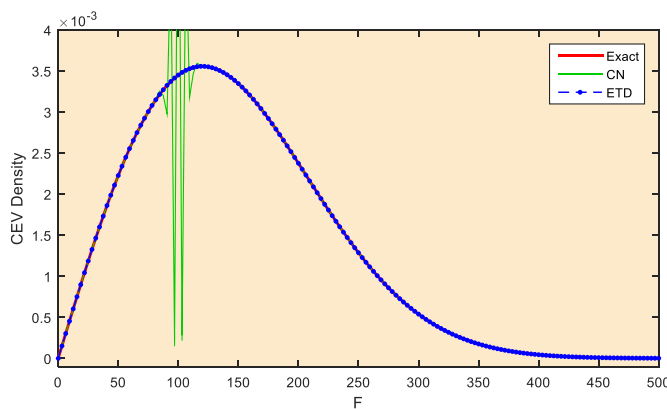


Figure 2. Computed CN, ETD and Exact Densities under CEV

Computed SABR Densities

The previous two examples demonstrated that the ETD scheme approximates the CEV and the Black-Scholes densities to a high degree of accuracy. The next numerical example computes the density function for the full SABR model with parameters $(\alpha_0, \beta, \rho, \nu) = (0.35, 0.25, -0.1, 1)$. The initial forward price $f=1$ is chosen and a maturity of $T = 1$ year, $r = 0$ and the test is performed with $F_{\max} = 5, M = 512$ and $N = 40$. Figure 3 shows the ETD solution is oscillation-free compared to the CN solution which exhibits oscillations near the initial forward price.

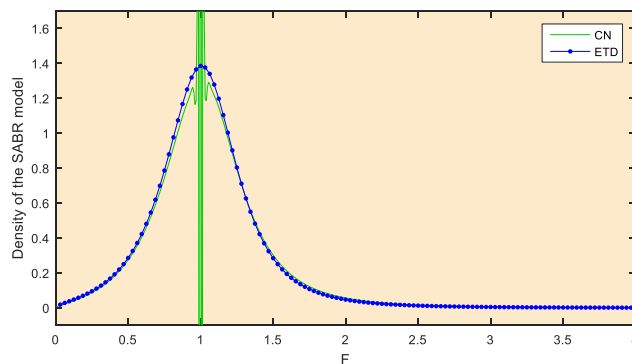


Figure 3. CN and ETD Densities under SABR

The next example compares computed density against the analytical approximation for the density given in Kienitz & Wetterau (2012, p. 397). The SABR model parameters are chosen as $(\alpha_0, \beta, \rho, \nu) = (0.4, 0.5, -0.06, 0.4)$ with an initial forward price of $f = 40$, $r = 0.05$ and $T = 0.5$ year. For this case, the test is performed using $F_{\max} = 80$, $M = 512$ and $N = 40$. From Figure 4, the same conclusion is reached as in the previous numerical example.

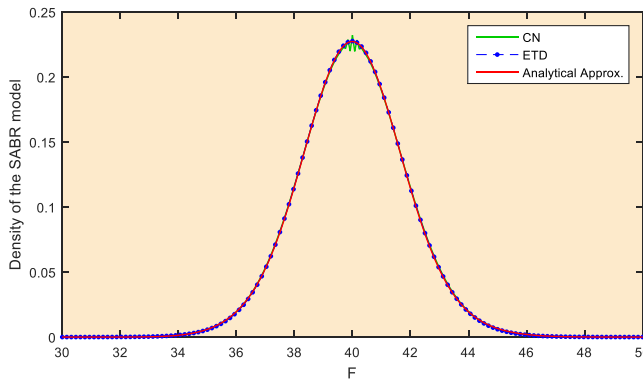


Figure 4. CN, ETD and Approximate Densities under SABR

The exponential time integration scheme has also been shown to suppress the wiggles at the strike prices for other pricing models (Rambeerich, Tangman, & Bhuruth, 2011). The proposed method will not produce oscillations whatever the choice of SABR parameters.

European Option Prices

The prices of European options can be obtained by computing the density function in (5). We start in a simpler case of a put option under the Black-Scholes model for the same set of parameters as in Hull (2006) with the current forward price $f = 20$, the exercise price $E = 20$ with a risk-free interest rate of $r = 0.09$ and the volatility of the forward price of $\alpha_0 = 0.25$. The numerical solutions arising by solving the density pde are given in Table 3. The exact option price is 1.11664.

Table 3
Option prices under the Black-Scholes Model

= 20, E = 20, r = 0.09, T = 4/12, $\alpha_0 = 0.25$				
1D-PDE ETD				
M	Price	Error	Rate	Cpu(s)
2^5	1.10985	6.8e-3	-	0.064
2^6	1.11462	2.0e-3	1.750	0.087
2^7	1.11611	5.3e-4	1.937	0.108
2^8	1.11651	1.3e-4	1.983	0.114
2^9	1.11662	3.3e-5	1.994	0.124
2^{10}	1.11663	8.4e-6	1.987	0.131
Exact	1.11664146			

Consider a European call option with a high at-the-money volatility of $\tilde{\sigma} = 0.5$, the current forward price as 100, an exercise price of 100 and $r = 0$ so that the forward price equals the stock price. Table 4 gives the computed prices using the ETD and the implied volatility approach (4) and the exact CEV formula (Schroder, 1989). Both the density approach and analytical approximation (4) which are denoted by HaganApprox are able to yield solutions with an error of 10^{-4} for different values of β for this small maturity problem.

Table 4
Call option prices under the CEV Model for $T=0.5$

$T = 0.5, f = 100, E = 100, r = 0, \tilde{\sigma} = 0.5, M = 2^9$					
β	Exact Price	Hagan Approx.		1D-PDE ETD	
		Price	Error	Price	Error
0	14.10474	14.10394	8.0e-4	14.10445	2.9e-4
0.3	14.06665	14.06706	4.1e-4	14.06637	2.8e-4
0.5	14.04931	14.04970	3.9e-4	14.04903	2.8e-4
0.7	14.03795	14.03813	1.8e-4	14.03747	4.8e-4

Lindsay & Brecher (2012) have priced European options under the CEV model using Monte Carlo simulations using the same parameters as in Table 4 for a long maturity of $T = 4$ years. We use this case to show that for the CEV model, the Hagan’s approximation results in a loss of accuracy.

From Table 5, we observe that the price computed by the Monte-Carlo approximations of Lindsay & Brecher and the density approach using ETD are in good agreement with the exact price even for a long maturity option while the Hagan & Woodward (1999) solutions lose accuracy when maturity increases.

Table 5
Call option prices under the CEV Model for $T=0.5$

$T = 4, f = 100, E = 100, r = 0, \sigma = 0.5, M = 2^9$						
B	Exact Price	Hagan Approx		1D-PDE ETD		Lindsay-Brecher Price
		Price	Error	Price	Error	
0	39.04516	39.75171	7.1e-1	39.04459	5.7e-4	39.04504 ± 0.05709
0.3	38.82097	39.00945	1.9e-1	38.81917	1.8e-3	38.82058 ± 0.06492
0.5	38.57528	38.65875	8.3e-2	38.57235	2.9e-3	38.57511 ± 0.07203
0.7	38.39279	38.42445	3.2e-2	38.38386	8.9e-3	38.39167 ± 0.08199

The numerical results for two special cases of the SABR model showed that the ETD method is more accurate than the implied volatility approach via Black’s formula. The results are convincing enough to claim that the ETD approach is an accurate technique that can be extended to the pricing of European options under the full SABR model. The author choose

$(\alpha, \beta, \rho, \nu) = (0.4, 0.5, -0.06, 0.4)$ with $F_{\max} = 80$ and an initial forward price of $f = 40$ and computes the price of a European put option with strike $E = 40$ and maturity $T = 0.5$. A numerical example show that the proposed method also works well for the general SABR model. For these parameters, both the Hagan implied volatility formula (3) and the fine-tuned formula (Oblój, 2008) gives $\sigma_B = 0.063659$.

Table 6
European put option prices under the SABR Model

Steps	$f = 40, E = 40, r = 0.05, \alpha_0 = 0.4, \beta = 0.5, \nu = 0.4, \rho = -0.06, T$							
	Monte Carlo				1D-PDE ETD			
	Price	Error	Cpu(s)	M	Price	Error	Rate	Cpu(s)
1000	0.70649	5.9e-3	8.729	2 ⁷	0.69723	3.3e-3	-	0.101
100000	0.70132	7.9e-4	591.3	2 ⁸	0.69963	8.9e-4	1.874	0.120
				2 ⁹	0.70028	2.4e-4	1.886	0.131
				2 ¹⁰	0.70045	7.1e-5	1.896	0.152
				2 ¹¹	0.70050	1.9e-5	1.744	0.169
				2 ¹²	0.70051	4.9e-6	1.887	0.197
Hagan's Approx = 0.70052,				Oblój's Approx = 0.70052				

Table 6 gives computed option prices using the density method and Monte Carlo simulations with 10^4 and 10^5 runs. The ETD requires 131 milliseconds to obtain a solution with an error of 10^{-4} while the Monte Carlo simulations require around 591 seconds. This shows that the proposed method is faster than existing methods and yields accurate prices.

CONCLUSION

A non-oscillatory scheme for computing a one-dimensional approximation of the SABR density was proposed. Numerical examples showed that option prices are computed to high accuracy. The methodology can be extended to the pricing of path dependent options such as barrier options and American options.

REFERENCES

- Andreasen, J., & Høge, B. N. (2012). ZABR -- *Expansions for the Masses*. Retrieved from <https://ssrn.com/abstract=1980726>.
- Antonov, A., Konikov, M., & Spector, M. (2013). SABR spreads its wings. *Risk*, 26(8), 58-63.
- Balland, P., & Tran, Q. (2013). SABR goes normal. *Risk*, 26(6), 72-77.
- Chang, C. C., Chung, S. L., & Stapleton, R. C. (2007). Richardson extrapolation techniques for the pricing of American-style options. *Journal of Futures Markets*, 27(8), 791-817.
- Cox, S. M., & Matthews, P. C. (2002). Exponential time differencing for stiff systems. *Journal of Computational Physics*, 176(2), 430-455.

- Hagan, P. S., Kumar, D., Lesniewski, A. S., & Woodward, D. E. (2002). Managing smile risk. In P. Wilmott (Ed.), *The Best of Wilmott 1: Incorporating the Quantitative Finance Review* (pp. 249-296). New York, NY: Wiley & Sons.
- Hagan, P. S., Kumar, D., Lesniewski, A., & Woodward, D. (2014). Arbitrage-Free SABR. *Wilmott*, 2014(69), 60-75.
- Hagan, P. S., & Woodward, D. E. (1999). Equivalent black volatilities. *Applied Mathematical Finance*, 6(3), 147-157.
- Hull, J. C. (2006). *Options, futures, and other derivatives* (6th Ed.). Upper Saddle River, N.J: Pearson/Prentice Hall.
- Kienitz, J., & Wetterau, D. (2012). *Financial modelling: theory, implementation and practice (with Matlab source)*. Chichester, West Sussex: Wiley.
- Lindsay, A. E., & Brecher, D. R. (2012). Simulation of the CEV process and the local martingale property. *Mathematics and Computers in Simulation*, 82(5), 868-878.
- Oblój, J. (2008). Fine-tune your smile: Correction to Hagan et al. *Wilmott Magazine*, 35, 102–104.
- Paulot, L. (2015). Asymptotic implied volatility at the second order with application to the SABR model. In P. K. Friz, J. Gatheral, A. Gulisashvili, A. Jacquier, & J. Teichmann (Eds.), *Large Deviations and Asymptotic Methods in Finance* (pp. 37-69). Cham, Switzerland: Springer International Publishing AG.
- Rambeerich, N., Tangman, D. Y., & Bhuruth, M. (2011). Numerical pricing of American options under infinite activity Lévy processes. *Journal of Futures Markets*, 31(9), 809-829.
- Schroder, M. (1989). Computing the constant elasticity of variance option pricing formula. *The Journal of Finance*, 44(1), 211-219.
- Tangman, D. Y., Thakoor, N., Dookhitram, K., & Bhuruth, M. (2011). Fast approximations of bond option prices under CKLS models. *Finance Research Letters*, 8(4), 206-212.
- Thakoor, N., Tangman, D. Y., & Bhuruth, M. (2013). A new fourth-order numerical scheme for option pricing under the CEV model. *Applied Mathematics Letters*, 26(1), 160-164.
- Thakoor, N., Tangman, D. Y., & Bhuruth, M. (2014). Efficient and high accuracy pricing of barrier options under the CEV diffusion. *Journal of Computational and Applied Mathematics*, 259, 182-193.
- Thakoor, N., Tangman, D. Y., & Bhuruth, M. (2015). Fast Valuation of CEV American Options. *Wilmott*, 2015(2015), 54-61.
- Trefethen, L. N., & Gutknecht, M. H. (1983). The Carathéodory–Fejér method for real rational approximation. *SIAM Journal on Numerical Analysis*, 20(2), 420-436.
- Trefethen, L. N. (2007). Evaluating matrix functions for exponential integrators via Carathéodory-Fejér approximation and contour integrals. *Electronic Transactions on Numerical Analysis*, 29, 1-18.